International Journal of Biological Macromolecules 165 (2020) 1455–1462

Contents lists available at ScienceDirect

International Journal of Biological Macromolecules

journal homepage: http://www.elsevier.com/locate/ijbiomac

Electrochemical sensing of cytochrome *c* using Graphene Oxide nanoparticles as platform

Bhawna Batra [a], Samiksha Sangwan [b], Jyoti Ahlawat [b], Minakshi Sharma [b,*]

[a] Department of Biotechnology, DCRUST, Murthal, Sonepat, Haryana, India
[b] Department of Zoology, Maharshi Dayanand University, Rohtak, Haryana, India

ARTICLE INFO

Article history:
Received 8 July 2020
Received in revised form 20 September 2020
Accepted 22 September 2020
Available online 01 October 2020

Keywords:
Cytochrome c oxidase
Cytochrome c (Cyt c) biosensor
Graphene oxide nanoparticles (GONPs)
Pencil graphite electrode
Blood serum

ABSTRACT

An improved cytochrome c (Cyt c) biosensor based on immobilization of cytochrome c oxidase (COx) on the surface of graphene oxide nanoparticles (GONPs) electrodeposited onto pencil graphite (PG) electrode. Characterization of graphene oxide nanoparticle was done by Transmission electron microscopy (TEM), Fourier transform infra-red spectroscopy (FTIR) and X-ray diffraction study (XRD). The working electrode (COx/GONPs/PG) was characterized at its different stages of fabrication by scanning electron microscopy (SEM) and FTIR. Fabrication of Cyt c biosensor was done by connecting COx/GONPs/PG as working electrode, Ag/AgCl as reference electrode and Pt as auxiliary electrode to potentiostat. The mechanism of detection of present biosensor was based on oxidation of Cyt c (reduced) to Cyt c (oxidized) by COx resulting in flow of electrons through GONPs to the PG electrode, hence current generated is proportional to the concentration of Cyt c. Present biosensor exhibited optimum potential at 0.49 V with optimum pH 7.5 and optimum temperature 35°C. Biosensor showed linearity within 40–180 ng/ml having 40 ng/ml limit of detection. The precision i.e. within and between-batch coefficients of variation (CVs) were found <0.04% and <0.21% respectively. The enzyme electrode lost 50% of its initial activity when operated for more than 6 months on weekly basis. It was applied for detection of Cyt c level in in apparently healthy and diseased human sera. The present biosensing method was co-related with standard colorimetric method and co-relation coefficient was found 0.99.

1. Introduction

The cytochrome complex or cytochrome c is a haemoprotein confined within inner mitochondrial membrane [1]. Cytochrome c is easily soluble in aqueous phase, and also a part of electron transport chain (ETC), where it works to transmit electrons between cytochrome *bc*1 complex (complex III) and cytochrome *c* oxidase (complex IV) of ETC [2]. It is competent to undertake oxidation and reduction reactions, without being attached with oxygen. Its main function is to catalyze the reduction of inspired oxygen to water in the terminal step of electron transport chain or rather we would say in the terminal step of respiration [3]. The detection of cytochrome is helpful for detection of myocardial infarction (MIs) [2] and cellular apoptosis [4]. MIs or heart attack, takes place when the heart muscles are subjected to ischemic conditions leading to tissue damage and concomitant release of cytochrome *c* thereby inducing apoptotic process and increased levels of cytochrome c in circulating blood. The normal level of cytochrome *c* in circulating blood is 39.8 ng/ml and elevated level at the time of myocardial infarction is up to 190 ng/ml [2]. That's why, measurement of serum level of cytochrome *c* is important for diagnosis of myocardial infarction. There are various methods to detect cytochrome *c* level in serum sample. Some of them are: electrochemiluminescence (ECL) [5], chemiluminescent [6], reverse phase – high performance liquid chromatography (HPLC) [7], ELISA (enzyme linked immunosorbent assay) [8], western blotting [9], immunoassay [10], scanning thermal lens microscope detection system [11] to name a few. These methods are highly responsive but have their some inherent limitations like involving a lot of physical work, more time-consuming, require specialist control.

To overcome drawbacks of these conventional methods, electrochemical methods [12] have been evolved to detect cytochrome *c* level due to their high reproducibility, high clarity, rapidity and longevity [13]. The basic principle of electrochemical biosensor lies in the fact that there is generation or utilization of electrons or ions in various reactions resulting in change of electrical properties of sample or solution, which can be recorded out and used as a parameter of measurement [12,14–16]. It is widely used to detect metabolites in a simple way with advancement in biosensor technology. Biosensor is an analytical device that uses the specificity and sensitivity of organic molecules in collaboration with electrochemical transducer to exhibit bio-analytical analysis with ease. Professor Leland C Clark Jnr (1918–2005) is regarded as father of

* Corresponding author.
E-mail addresses: sminakshi.2007@rediffmail.com, sminakshi541@gmail.com (M. Sharma).

https://doi.org/10.1016/j.ijbiomac.2020.09.203
0141-8130/

biosensor. Biosensors can be classified on the basis of transducer, into following five types: electrochemical biosensor (amperometric biosensor and potentiometric biosensor), ion-sensitive biosensor, piezoelectric biosensor, optical biosensor, conductometric biosensor [17–27]. But many lacuna still exists which are to be addressed such as lower stability, longer response time, lower reproducibility and higher working electrode potential.

Nanoparticles are used to directly convey electron between enzyme and electrode for the development of third generation biosensors now a days. The pencil graphite (PG) electrodes are widely used for immobilization of enzyme [28]. PG electrode is widely used due to their distinctive properties such as high electrical conductivity, inherent strength, elasticity etc. In current years, graphene oxide nanoparticles (GONPs) have been used in many researches [29,30] due to its larger surface area to mass ratio which makes it an excellent material for use in energy storage or chemical sensing and they have been used in production of bio- devices and optoelectronics, and for use in drug delivery [31–33]. We describe here, construction and application of cytochrome *c* biosensor based on immobilization of COx onto GONPs electrodeposited on the surface of PG electrode.

2. Materials and methods

2.1. Materials

Cytochrome c oxidase from Sigma Aldrich, graphite flakes, sodium nitrate ($NaNO_3$), potassium permagnate ($KMnO_4$), hydrogen peroxide (H_2O_2), hydrogen chloride (HCl), deionised water, potassium chloride (KCl), potassium dihydrogen phosphate (K_2HPO_4), tris, tris HCl, acetate, acetic acid (CH_3COOH), 4-aminophenazone, solid phenol, horse-radish peroxidise, sulphuric acid (H_2SO_4), silica, ascorbic acid, cytochrome *c*, potassium ferricyanide, sucrose.

2.2. Apparatus

Poentiostat/galvanostat (Make: Autolab, model AUT83785, manufactured by Ecochemie) with a three electrode system consisting of a Platinum wire as an auxiliary electrode, an Ag/AgCl electrode in 3.5 M KCl as reference electrode and cytochrome c oxidase/GONPs altered pencil graphite electrode as a working electrode. Transmission electron microscope (TEM) (Zeiss EV040), XRD (make: 122 Rigaku D/Max 2550, Tokyo Japan), Fourier transform infra-red spectroscopy (FTIR) (Bruker).

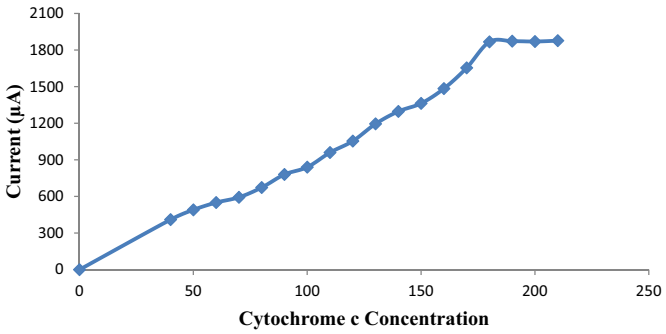

Fig. 2. Hyperbolic curve for cytochrome c biosensor for effect of cytochrome *c* concentration on response of cytochrome *c* biosensor based on GONPs/PG electrode bound cytochrome *c* oxidase.

2.3. Assay of cytochrome c oxidase (COx)

Free cytochrome *c* assay was done by slight changes in Satyapal and Pundir process of assay. Cyt c 1.0% (w/v) solution was prepared in potassium phosphate buffer (10 mM, pH 7.0). 3–5 mg of ascorbic acid used to reduce solution. Reaction mixture containing 2.7 ml of phosphate buffer (10 mM, pH 7.0) and 0.2 ml of Cyt c was incubated at 37 °C for 10 min. The reaction starts by adding 0.1 ml of COx solution (0.1 mg solid/ml) while in blank in place of COx, 0.1 ml of potassium ferricyanide (100 mM, in phosphate buffer) is used. It was mixed by inversion and the decrease in A550 nm was monitored for 10 min at interval of 1 min.

$$\Delta E = E_t - E_f$$

E_t = A550nm value at the time points 0 through 10 min for the test

E_f = A550nm value at the 10 min time point for the blank.

One unit will oxidize 1.0 µmol of reduced cytochrome *c* to oxidized cytochrome *c* (using 0.5 µmol of oxygen) per minute at pH 7.0 at 37 °C.

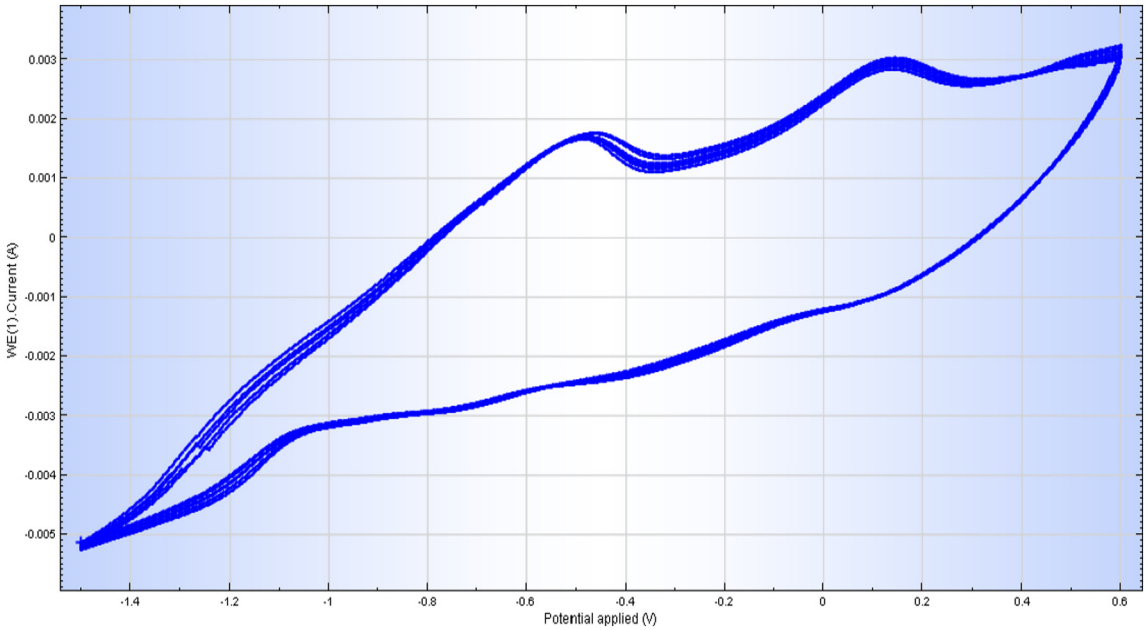

Fig. 1. Cyclic voltammogram for electrodeposition of GONPs. Supporting electrolyte: 1 M KCl solution; scan rate: 25 mV/s.

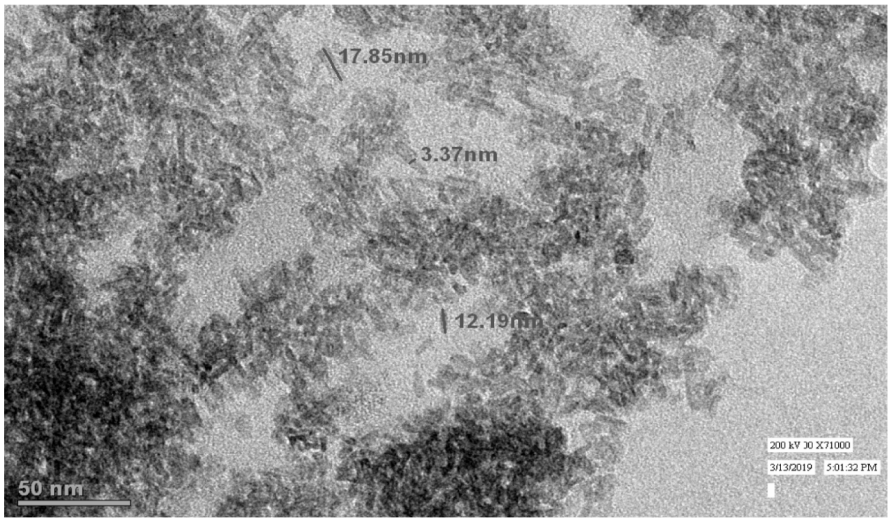

(a)

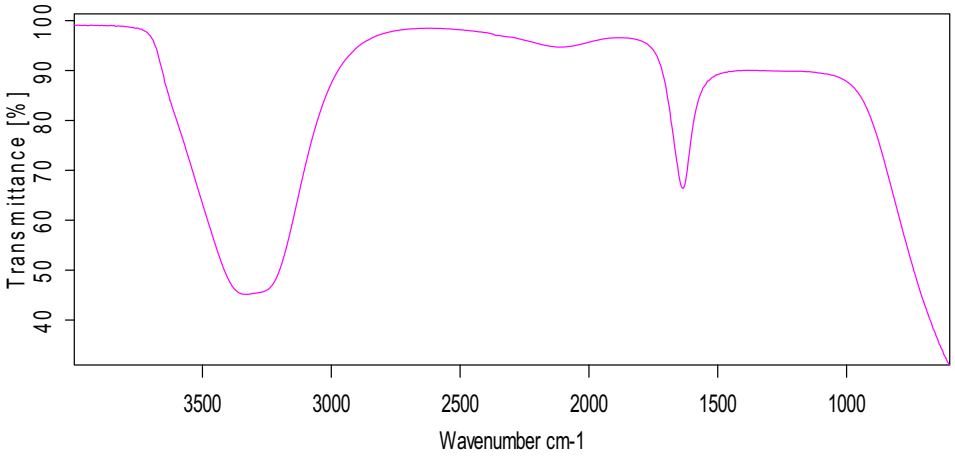

(b)

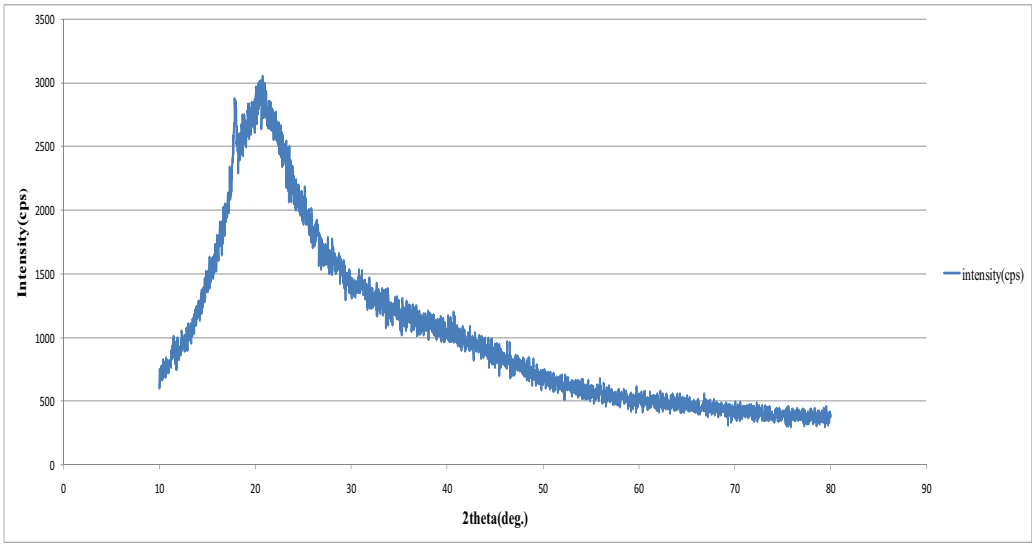

(c)

Fig. 3. (a) Transmission electron microscope (TEM) images, of GO-NPs, (b) FTIR spectrum of GONPs and (c) X-ray diffraction (XRD) pattern of GONPs.

2.4. Preparation of GONPs

GO nanoparticles were prepared using modified Hummer's method. Firstly, 500 mg of graphene powder and 500 mg of sodium nitrate were mixed in 25 ml of 18.4 M sulphuric acid (98%). Magnetically stir mixture for 15 min in ice bath. After that, 4 g of potassium permagnate was added slowly at 20°C temperature. Mix 50 ml double distilled water slowly and magnetically stirred for 90 min at 40°C temperature. Formation of brown suspension occurred. Treat suspension with 6 ml of 30% H_2O_2 solution followed by dilution with 50 ml deionised water. 5% HCl used to wash suspension. To attain neutrality, treat solution with deionised water to discard enough of manganese salt. Dried remaining solution in oven for 1 h. Dry GONPs were formed and their structural properties studied.

2.5. Characterization of GONPs

Characterization of GONPs was done by transmission electron microscopy (TEM), Fourier transform infra-red spectroscopy (FTIR) & X-ray diffraction (XRD) which confirmed its synthesis.

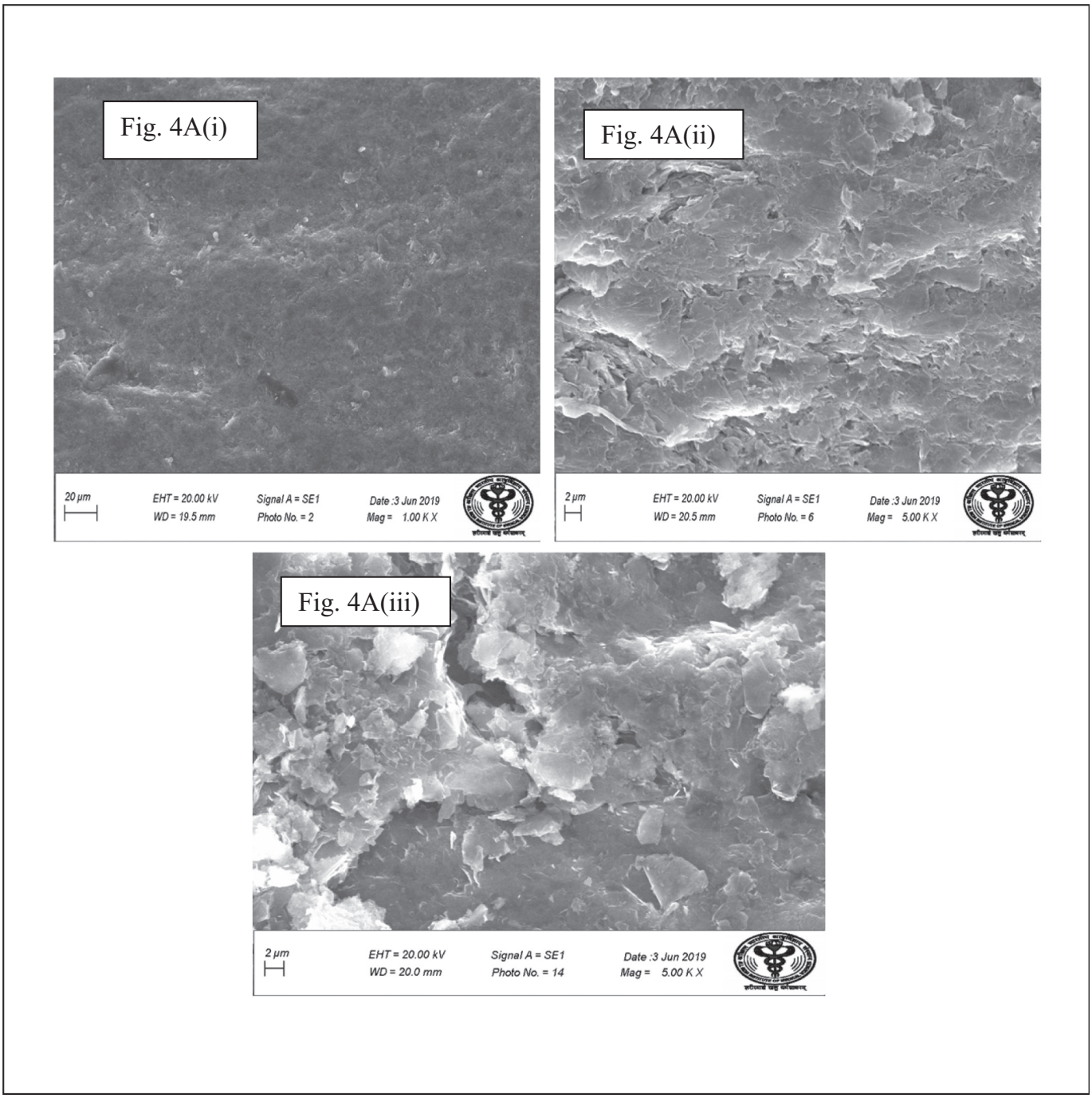

Fig. 4. A SEM images of (i) Bare PG electrode, (ii) GONPs/PG electrode and (iii) COx/GO-NPs/PG electrode. B: Fourier transform infra-red spectroscopy (FTIR) of (i) bare PG electrode, (ii) GONPs/PG electrode and (iii) COx/GONPs/PG electrode.

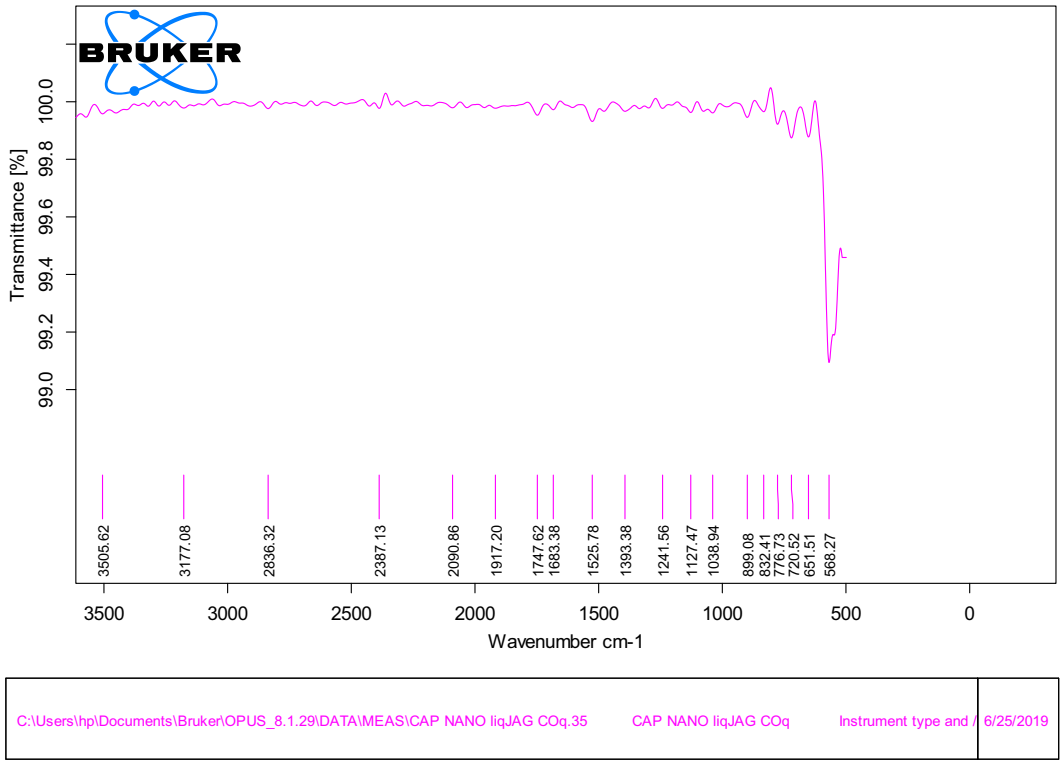

Fig. 4 (*continued*).

2.6. Electrodeposition of GONPs on PG electrode

Alumina slurry used to polish surface of PG electrode (2 cm × 2 mm) to soften it. A mixture of 4 ml of H_2SO_4: HCl (3:1 ratio) is prepared and PG electrode is dipped in it for some time. GONPs (200 μl) were added to 25 ml of 1M KCl. Electrodeposition of GONPs onto PG electrode by operating 5 polymerization cycles at −1.50V to 0.60V was possessed in an electrochemical cell system using Autolab. Finally, unbound matter

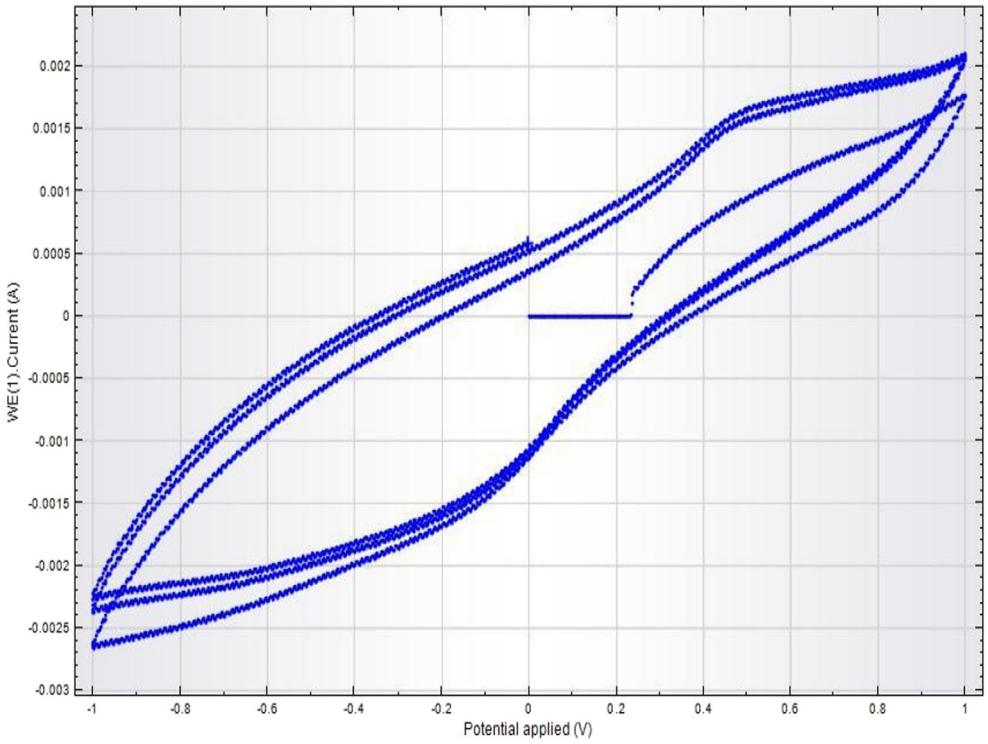

Fig. 5. Cyclic voltammetry response of COx/GONPs/PG on successive addition of 100 μl cytochrome *c* in 25 ml 0.1 phosphate buffer (pH = 7.5) at the different potential at a scan rate of 25 mV/s.

removed by distilled water sponge from GONPs PG electrode and placed at 4°C in petriplate (Fig. 1).

2.7. Immobilization of COx onto GONPs modified PG electrode

Mixture of 0.2 ml of COx and 1.8 ml of 10 mM potassium phosphate buffer of pH 7.0 was placed onto surface of GONPs/PG electrode. This is placed for immobilization at 4°C temperature. Immobilized CO_x electrode now washed for 3–4 times with 10 mM potassium phosphate buffer (pH 7.0). The resulting COx/GONPs/PG electrode was used as a working electrode. When not in use it was preserved at 4°C.

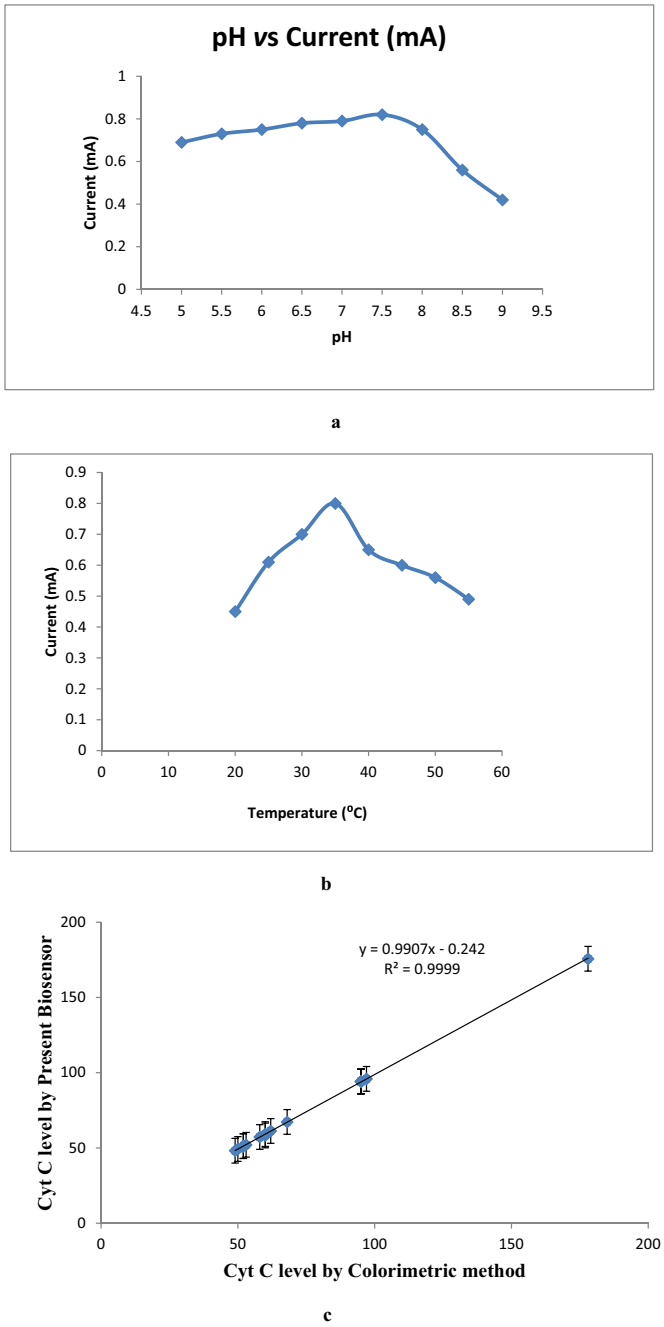

Fig. 6. (a) Effect of pH on COx/GONPs/PG electrode, (b) effect of temperature on COx/GONPs/PG electrode (c) co-relation study of present biosensor with standard colorimetric method.

Characterization of working electrode is done by SEM in distinct period of construction.

2.8. Characterization of COx/GONPs/PG electrode

Scanning electron microscopy (SEM) and Fourier transform infrared spectroscopy (FTIR) used to characterize working PG electrode at different stages.

2.9. Fabrication of cytochrome c biosensor

By using three electrode cell systems, composed of CO_x/GONPs/PG as working electrode, silver/silver chloride (Ag/AgCl) as reference electrode and Platinum wire as auxiliary electrode an amperometric cytochrome *c* biosensor set up. All three electrodes attached by potentiostat galvanostat.

2.10. Optimization of cytochrome c biosensor

Optimization of biosensor was done by altering temperature, pH and substrate concentration. Check response of changing condition on biosensor. By using three types of buffer of 0.1M concentration, pH varied between 5 and 9 pH at an interval of 0.5. For 5 to 6 acetate buffer, 6.5 to 7.5 potassium phosphate buffer and 8 to 9 was of Tris-HCl buffer used. A range of 20.0°C–50.0°C temperature used to check temperature effect on biosensor. Similarly a range of 40 ng/ml to 210 ng/ml was used to check cytochrome *c* concentration difference on biosensor response.

3. Results and discussion

3.1. Characterization of GONPs

TEM, XRD and FTIR are used to characterize nanoparticles. Transmission electron microscope images of GO nanoparticles are of rod shaped. The average size of one GrO nanoparticle was to be nearly 50 nm (Fig. 3a). The XRD pattern of graphene nanoparticle showed the presence of a sharp diffraction peak at $2\Theta = 25.0$ °C, indicating that GO nanoparticle existed independently in extremely biased manner (Fig. 3b). FTIR spectra of 1550.0 and 1190.0 cm^{-1} corresponding to C═C conjugation and C—C band stretching vibrations in GONPs. FTIR spectra do not show any peak relevant to oxygen that means after reduction of GO, oxygen comprising functional group lost. Peak at 3400 cm^{-1}, 1600 cm^{-1} and 1060 cm^{-1} because of O—H stretching, C═C stretching and C—O stretching respectively (Fig. 3c).

3.2. Characterization of COx/GONPs/PG electrode by scanning electron microscopy (SEM) & Fourier transform infra-red spectroscopy (FTIR)

SEM images of bare (Fig. 4A (i)) and working (COx/GONPs/PG) electrode confirmed the fabrication of electrode. SEM image of GONPs/PG (ii) exhibited spherical shapes of nanoparticles on the surface of electrode, hence established the electrodeposition of GONPs onto PG. SEM image of COx/GONPs/PG (iii) revealed the presence of globular structures onto GONPs/PG, thus confirmed the immobilization of Cox. FTIR spectra of COx/GONPs/PG enzyme electrode were presented by the peaks at 3505.62 cm^{-1}, 3177.08 cm^{-1}, 2836.32 cm^{-1}, 2387.13 cm^{-1}, 2090.96 cm^{-1}, 1917.20 cm^{-1}, 1747.62 cm^{-1}, 1525.78 cm^{-1}, 1038.94 cm^{-1}, 651.51 cm^{-1}, 568.27 cm^{-1} equivalent to O—H stretching, C═C bond and C═O (Fig. 4B(iii)).

3.3. Cyclic voltammetric measurement

Cyclic voltammogram (CV) of COx/GONPs/PG electrode was recorded in potentiostat-galvanostat from −1.5V to 0.6V in a 25.0 ml of 10.0 mM potassium phosphate buffer (pH 7.0) containing 100.0 μl

cytochrome c. An electrochemical reaction happens during response quantification:

$$4\,\mathrm{Cyt\,c}\left(\mathrm{Fe}^{+2}\right) + 2O_2 + 4H_2O \overset{CO_x}{\rightarrow} 4\,\mathrm{Cyt\,c}\left(\mathrm{Fe}^{+3}\right) + 4H_2O_2$$

$$4H_2O_2 \overset{0.49\,V}{\rightarrow} 8H^+ + 8e^- + 4O_2$$

$$8e^- \overset{GONPs}{\rightarrow} \mathrm{PG\,electrode}$$

For high responsiveness and fast sensor operation, 0.49 V was chosen as the most advantageous working potential for cytochrome c detection in this work (Fig. 5).

3.4. Optimization of experimental conditions

Biosensor response was affected by change in temperature, pH and substrate (Cyt c) concentration. The optimum current was obtained at pH 7.5 (Fig. 6a), temperature 35°C (Fig. 6b) and linearity for substrate concentration found 40–180 ng/ml comparable to existing cytochrome c biosensor (Fig. 2).

3.5. Evaluation of the biosensor

The performance of this biosensor was evaluated by following parameters.

3.5.1. Reproducibility

Within and between-batch coefficients of variation for the determination of cytochrome *c* in sera on the same day and after one week of storage were <0.04% and <0.21%, respectively. These high precisions highlighted the good reproducibility and consistency of the present biosensor (Table 1). This can be attributed to the covalent immobilization of COx onto GONPs modified PG electrode.

3.5.2. Repeatability

To reuse the working electrode, it was washed by dipping it in 10 mM, pH 7.0 potassium phosphate buffer (PB) solution 3–4 times at room temperature. 50% of enzyme electrode initial activity lost when assay operate for more than 6 months in weekly basis which showed that GONPs composite film has better biocompatibility. The biological activity of the immobilized enzyme was also maintained. The enzyme electrode preserved at 4 °C in dried condition when not in use.

Table 1
Within and between batches assay co-efficient of variation (CVs) for determination of cytochrome *c* levels in serum by biosensor employing cytochrome *c* oxidase GONPs/PG composite film.

Total number of serum samples (n = 6)	Mean serum cytochrome *c* (ng/ml)	%CV
Within batch(6)		
50.1	50.2	0.04%
50		
50.4		
50.3		
50.1		
50.1		
Between batch(6)		
150	149.5	0.21%
149.5		
149		
150.5		
148.9		
149.2		

Table 2
Serum cytochrome *c* levels in apparently healthy persons and cardiac patients, as measured by cytochrome *c* biosensor based on cytochrome *c* oxidase GONPs/PG composite film.

S. no.	Sex	Age (year)	Cyt C serum level(ng/ml)
1	Male	58	60
2	Male	65	95
3	Female	50	97
4	Male	52	95
5	Male	62	95
6	Female	60	178
7	Male	80	95
8	Male	34	50
9	Male	40	62
10	Male	65	68
11	Male	46	52
12	Female	59	58
13	Male	70	53
14	Male	52	52
15	Male	48	49
16	Male	51	60

3.5.3. Correlation study

The present biosensor was correlated with standard colorimetric assay for cytochrome *c* and coefficient of correlation was found $R^2 = 0.999$ (Fig. 6c).

3.6. Application of cytochrome c biosensor in sera

Serum samples (1ml each) were drawn from diseased persons having myocardial infarction at Pt. Bhagwat Dayal Sharma Post Graduate Institute of Medical Sciences, Rohtak. Determination of cytochrome *c* content in serum sample was carried out in similar way as described above, by providing optimal condition of working (Table 2). Here, serum sample of cardiac patient used instead of cytochrome *c*. A hyperbolic curve made between cytochrome *c* concentration and current (μA) to interpolate cytochrome *c* content in serum samples.

4. Conclusion

An improved cytochrome *c* biosensor has been developed by using graphene oxide nanoparticles (GONPs) electrodeposited onto the surface of PG electrode. This cytochrome *c* biosensor was constructed using COx/GONPs/PG electrode as working electrode, Ag/AgCl as standard or reference and Platinum wire as auxiliary electrode connected through potentiostat/galvanostat. GONPs were prepared by using Hummer's method. This present cytochrome c biosensor has been utilized to determine cytochrome *c* level in serum samples.

Declaration of competing interest

The authors declare that there is no conflict of interest among the authors.

References

[1] C. Guo, J. Wang, X. Chen, Y. Li, L. Wu, J. Zhang, et al., Construction of a biosensor based on a combination of cytochrome c, graphene, and gold nanoparticles, Sensors 19 (2018) 40, https://doi.org/10.3390/s19010040.
[2] B. Batra, S. Lata, S. Rani, C.S. Pundir, Fabrication of a cytochrome c biosensor based on cytochrome oxidase/NiO-NPs/cMWCNT/PANI modified Au electrode, J. Biomed. Nanotechnol. 9 (2013) 409–416, https://doi.org/10.1166/jbn.2013.1549.
[3] Y. Song, H. Liu, L. Wan, Y. Wang, H. Hou, L. Wang, Direct electrochemistry of cytochrome c based on poly(diallyldimethylammonium chloride)-graphene nanosheets/gold nanoparticles hybrid nanocomposites and its biosensing, Electroanalysis 25 (2013) 1400–1409, https://doi.org/10.1002/elan.201200524.

[4] K. Matsuura, K. Canfield, W. Feng, M. Kurokawa, Metabolic regulation of apoptosis in cancer, Int. Rev. Cell Mol. Biol. (2016) 43–87, https://doi.org/10.1016/bs.ircmb.2016.06.006.
[5] M.R.K. Pur, M. Hosseini, F. Faridbod, A.S. Dezfuli, M.R. Ganjali, A novel solid-state electrochemiluminescence sensor for detection of cytochrome c based on ceria nanoparticles decorated with reduced graphene oxide nanocomposite, 408, 2016 7193–7202, https://doi.org/10.1007/s00216-016-9856-6.
[6] M. Aizawa, Y. Ikariyama, H. Kuno, Photovoltaic determination of hydrogen peroxide with a biophotodiode, Anal. Lett. 17 (1984) 555–564, https://doi.org/10.1080/00032718408066489.
[7] S.I. Dikalov, D.G. Harrison, Methods for detection of mitochondrial and cellular reactive oxygen species, Antioxid. Redox Signal. 20 (2014) 372–382, https://doi.org/10.1089/ars.2012.4886.
[8] K. Barczyk, M. Kreuter, J. Pryjma, E.P. Booy, S. Maddika, S. Ghavami, et al., Serum cytochrome c indicatesin vivo apoptosis and can serve as a prognostic marker during cancer therapy, Int. J. Cancer 116 (2005) 167–173, https://doi.org/10.1002/ijc.21037.
[9] M. Tafani, N.O. Karpinich, K.A. Hurster, J.G. Pastorino, T. Schneider, M.A. Russo, et al., Cytochrome c release upon Fas receptor activation depends on translocation of full-length bid and the induction of the mitochondrial permeability transition, J. Biol. Chem. 277 (2002) 10073–10082, https://doi.org/10.1074/jbc.m111350200.
[10] J.-M. Liu, X.-P. Yan, Ultrasensitive, selective and simultaneous detection of cytochrome c and insulin based on immunoassay and aptamer-based bioassay in combination with Au/Ag nanoparticle tagging and ICP-MS detection, J. Anal. At. Spectrom. 26 (2011) 1191, https://doi.org/10.1039/c0ja00232a.
[11] E. Tamaki, K. Sato, M. Tokeshi, K. Sato, M. Aihara, T. Kitamori, Single-cell analysis by a scanning thermal lens microscope with a microchip: direct monitoring of cytochrome c distribution during apoptosis process, Anal. Chem. 74 (2002) 1560–1564, https://doi.org/10.1021/ac011092t.
[12] H. Karimi-Maleh, Omotayo, A. Arotiba, Simultaneous determination of cholesterol, ascorbic acid and uric acid as three essential biological compounds at a carbon paste electrode modified with copper oxide decorated reduced graphene oxide nanocomposite and ionic liquid, J. Colloid Interface Sci. 560 (2020) 208–212, https://doi.org/10.1016/j.jcis.2019.10.007.
[13] S. Lata, B. Batra, N. Karwasra, C.S. Pundir, An amperometric H2O2 biosensor based on cytochrome c immobilized onto nickel oxide nanoparticles/carboxylated multiwalled carbon nanotubes/polyaniline modified gold electrode, Process Biochem. 47 (2012) 992–998, https://doi.org/10.1016/j.procbio.2012.03.018.
[14] Y. Liu, N. Song, Z. Ma, K. Zhou, Z. Gan, Y. Gao, et al., Synthesis of a poly(N-methylthionine)/reduced graphene oxide nanocomposite for the detection of hydroquinone, Mater. Chem. Phys. 223 (2019) 548–556, https://doi.org/10.1016/j.matchemphys.2018.11.045.
[15] Z. Shamsadin-Azad, M.A. Taher, S. Cheraghi, H. Karimi-Maleh, A nanostructure voltammetric platform amplified with ionic liquid for determination of tert-butylhydroxyanisole in the presence kojic acid, J. Food Meas. Charact. 13 (2019) 1781–1787, https://doi.org/10.1007/s11694-019-00096-6.
[16] S. Zhu, R. Chen, W. Zhang, X. Niu, W. Chen, L. Mo, et al., Dissecting terminal fluorinated regulator of liquid crystals for fine-tuning intermolecular interaction and molecular configuration, J. Mol. Liq. 310 (2020), 113225, https://doi.org/10.1016/j.molliq.2020.113225.
[17] M. Baghayeri, R. Ansari, M. Nodehi, I. Razavipanah, H. Veisi, Label-free electrochemical bisphenol A aptasensor based on designing and fabrication of a magnetic gold nanocomposite, Electroanalysis 30 (2018) 2160–2166, https://doi.org/10.1002/elan.201800158.
[18] M. Baghayeri, R. Ansari, M. Nodehi, I. Razavipanah, H. Veisi, Voltammetric aptasensor for bisphenol A based on the use of a MWCNT/Fe3O4@gold nanocomposite, Microchim. Acta 185 (2018)https://doi.org/10.1007/s00604-018-2838-y.
[19] M. Baghayeri, R. Ansari, M. Nodehi, H. Veisi, Designing and fabrication of a novel gold nanocomposite structure: application in electrochemical sensing of bisphenol A, Int. J. Environ. Anal. Chem. 98 (2018) 874–888, https://doi.org/10.1080/03067319.2018.1512595.
[20] M. Baghayeri, M. Ghanei-Motlagh, R. Tayebee, M. Fayazi, F. Narenji, Application of graphene/zinc-based metal-organic framework nanocomposite for electrochemical sensing of As(III) in water resources, Anal. Chim. Acta 1099 (2020) 60–67, https://doi.org/10.1016/j.aca.2019.11.045.
[21] M. Ghanei-Motlagh, M.A. Taher, M. Fayazi, M. Baghayeri, A. Hosseinifar, Non-enzymatic amperometric sensing of hydrogen peroxide based on vanadium pentoxide nanostructures, J. Electrochem. Soc. 166 (2019)https://doi.org/10.1149/2.0521906jes.
[22] H. Karimi-Maleh, K. Cellat, K. Arıkan, A. Savk, F. Karimi, F. Şen, Palladium–nickel nanoparticles decorated on functionalized-MWCNT for high precision non-enzymatic glucose sensing, Mater. Chem. Phys. 250 (2020), 123042, https://doi.org/10.1016/j.matchemphys.2020.123042.
[23] H. Karimi-Maleh, K. Cellat, K. Arıkan, A. Savk, F. Karimi, F. Şen, Palladium–nickel nanoparticles decorated on functionalized-MWCNT for high precision non-enzymatic glucose sensing, Mater. Chem. Phys. 250 (2020), 123042, https://doi.org/10.1016/j.matchemphys.2020.123042.
[24] H. Karimi-Maleh, F. Karimi, M. Alizadeh, A.L. Sanati, Electrochemical sensors, a bright future in the fabrication of portable kits in analytical systems, Chem. Rec. 20 (2020)https://doi.org/10.1002/tcr.201900092.
[25] H. Karimi-Maleh, F. Karimi, S. Malekmohammadi, N. Zakariae, R. Esmaeili, S. Rostamnia, M. LütfiYola, N. Atar, S. Movaghgharnezhad, S. Rajendran, A. Razmjou, Y. Orooji, S. Agarwal, V. Kumar Gupta, An amplified voltammetric sensor based on platinum nanoparticle/polyoxometalate/two-dimensional hexagonal boron nitride nanosheets composite and ionic liquid for determination of N-hydroxysuccinimide in water samples, J. Mol. Liq. 310 (2020) 113185, https://doi.org/10.1016/j.molliq.2020.113185.
[26] H. Karimi-Maleh, M. Shafieizadeh, M.A. Taher, F. Opoku, E. Muriithi Kiarii, P. Penny Govender, S. Ranjbari, M. Rezapour, Y. Orooji, The role of magnetite/graphene oxide nano-composite as a high-efficiency adsorbent for removal of phenazopyridine residues from water samples, an experimental/theoretical investigation, J. Mol. Liq. 298 (15 January 2020) 112040, https://doi.org/10.1016/j.molliq.2019.112040.
[27] M. Rouhi, M.M. Lakouraj, M. Baghayeri, Low band gap conductive copolymer of thiophene with p-phenylenediamine and its magnetic nanocomposite: synthesis, characterization and biosensing activity, Polym. Compos. 40 (2018) 1034–1042, https://doi.org/10.1002/pc.24790.
[28] J.-F. Wu, M.-Q. Xu, G.-C. Zhao, Graphene-based modified electrode for the direct electron transfer of Cytochrome c and biosensing, Electrochem. Commun. 12 (2010) 175–177, https://doi.org/10.1016/j.elecom.2009.11.020.
[29] C. Chen, Z. Gan, K. Zhou, Z. Ma, Y. Liu, Y. Gao, Catalytic polymerization of N-methylthionine at electrochemically reduced graphene oxide electrodes, Electrochim. Acta 283 (2018) 1649–1659, https://doi.org/10.1016/j.electacta.2018.07.051.
[30] Z. Gan, N. Song, H. Zhang, Z. Ma, Y. Wang, C. Chen, One-step electrofabrication of reduced graphene oxide/poly(N-methylthionine) composite film for high performance supercapacitors, J. Electrochem. Soc. 167 (2020), 085501, .
[31] A. Khodadadi, E. Faghih-Mirzaei, H. Karimi-Maleh, A. Abbaspourrad, S. Agarwal, V.K. Gupta, A new epirubicin biosensor based on amplifying DNA interactions with polypyrrole and nitrogen-doped reduced graphene: experimental and docking theoretical investigations, Sensors Actuators B Chem. 284 (2019) 568–574, https://doi.org/10.1016/j.snb.2018.12.164.
[32] J. Mohanraj, D. Durgalakshmi, R. Ajay Rakkesh, S. Balakumar, Saravanan Rajendran, H. Karimi-Maleh, Facile synthesis of paper based graphene electrodes for point of care devices: a double stranded DNA (dsDNA) biosensor, J. Colloid Interface Sci. 566 (2020) 463–472, https://doi.org/10.1016/j.jcis.2020.01.089.
[33] F. Tahernejad-Javazmi, M. Shabani-Nooshabadi, H. Karimi-Maleh, 3D reduced graphene oxide/FeNi3-ionic liquid nanocomposite modified sensor; an electrical synergic effect for development of tert-butylhydroquinone and folic acid sensor, Compos. Part B 172 (2019) 666–670, https://doi.org/10.1016/j.compositesb.2019.05.065.